

Spontaneous Charge Current in a Doped Weyl Semimetal

Yositake Takane

*Department of Quantum Matter, Graduate School of Advanced Sciences of Matter,
Hiroshima University, Higashihiroshima, Hiroshima 739-8530, Japan*

(Received)

A Weyl semimetal hosts low-energy chiral surface states, which appear to connect a pair of Weyl nodes in reciprocal space. As these chiral surface states propagate in a given direction, a spontaneous circulating current is expected to appear near the surface of a singly connected Weyl semimetal. This possibility is examined by using a simple model with particle-hole symmetry. It is shown that no spontaneous charge current appears when the Fermi level is located at the band center. However, once the Fermi level deviates from the band center, a spontaneous charge current appears to circulate around the surface of the system and its direction of flow is opposite for the cases of electron doping and hole doping. These features are qualitatively unchanged even in the absence of particle-hole symmetry. The circulating charge current is shown to be robust against weak disorder.

1. Introduction

A Weyl semimetal possesses a pair of, or pairs of, non-degenerate Dirac cones with opposite chirality.^{1–10)} The pair of Dirac cones can be nondegenerate if time-reversal symmetry or inversion symmetry is broken. The electronic property of a Weyl semimetal is significantly influenced by the position of a pair of Weyl nodes in reciprocal and energy spaces, where a Weyl node represents the band-touching point of each Dirac cone. In the absence of time-reversal symmetry, a pair of Weyl nodes is separated in reciprocal space. In this case, low-energy states with chirality appear on the surface of a Weyl semimetal³⁾ if the Weyl nodes are projected onto two different points in the corresponding surface Brillouin zone. A notable feature of such chiral surface states is that they propagate only in a given direction, which depends on the position of the Weyl nodes. This gives rise to an anomalous Hall effect.⁵⁾ If inversion symmetry is also broken in addition to time-reversal symmetry, a pair of Weyl nodes is also separated in energy space. In this case, the propagating direction of chiral surface states is tilted according to the deviation of the Weyl nodes. If only inversion symmetry is broken, no chiral surface state appears since the pair of Weyl nodes coincides in reciprocal space. To date, some materials have been experimentally identified as Weyl semimetals.^{11–18)}

Let us focus on the case in which a Weyl semimetal with a pair of Weyl nodes at $\mathbf{k}_{\pm} = (0, 0, \pm k_0)$ is in the shape of a long prism parallel to the z axis. In this case, chiral surface states appear on the side of the system. In the presence of inversion symmetry, they typically propagate in a direction perpendicular to the z axis; thus, we expect that a spontaneous charge current appears to circulate in the system near the side surface. If inversion symmetry is additionally broken, the propagating direction is tilted to the z direction; thus, an electron in the chiral surface state shows spiral motion around the system.¹⁹⁾ Thus, we expect that a spontaneous charge current has a nonzero component in the z direction. This longitudinal component must be canceled out by the con-

tribution from bulk states if they are integrated over a cross section parallel to the xy plane.

In this paper, we theoretically examine whether a spontaneous charge current appears in the ground state of a Weyl semimetal. Our attention is focused on the case where time-reversal symmetry is broken. We calculate the spontaneous charge current induced near the side of the system by using a simple model with particle-hole symmetry. We find that no spontaneous charge current appears when the Fermi level, E_F , is located at the band center, which is set equal to 0 hereafter, implying that the contribution from chiral surface states is completely canceled out by that from bulk states. However, once E_F deviates from the band center, the spontaneous charge current appears to circulate around the side surface of the system and its direction of flow is opposite for the cases of electron doping (i.e., $E_F > 0$) and hole doping (i.e., $E_F < 0$). The circulating charge current is shown to be robust against weak disorder. In the absence of inversion symmetry, we show that chiral surface states induce the longitudinal component of a spontaneous charge current near the side surface, which is compensated by the contribution from bulk states appearing beneath the side surface. This longitudinal component is shown to be fragile against disorder.

In the next section, we present a tight-binding model for Weyl semimetals and show the absence of a spontaneous charge current when the Fermi level is located at the band center. In Sect. 3, we derive a tractable continuum model from the tight-binding model and analytically determine the magnitude of a spontaneous charge current induced by the deviation of the Fermi level from the band center. In Sect. 4, we numerically study the behaviors of a spontaneous charge current by using the tight-binding model. We also examine the effect of disorder on the spontaneous charge current. The last section is devoted to a summary and discussion. We set $\hbar = 1$ throughout this paper.

2. Model

Let us introduce a tight-binding model for Weyl semimetals on a cubic lattice with lattice constant a . Its Hamiltonian is given by $H = H_0 + H_x + H_y + H_z$ with^{4,5)}

$$H_0 = \sum_{l,m,n} |l, m, n\rangle h_0 \langle l, m, n|, \quad (1)$$

$$H_x = \sum_{l,m,n} \{|l+1, m, n\rangle h_x \langle l, m, n| + \text{h.c.}\}, \quad (2)$$

$$H_y = \sum_{l,m,n} \{|l, m+1, n\rangle h_y \langle l, m, n| + \text{h.c.}\}, \quad (3)$$

$$H_z = \sum_{l,m,n} \{|l, m, n+1\rangle h_z \langle l, m, n| + \text{h.c.}\}, \quad (4)$$

where the indices l , m , and n are respectively used to specify lattice sites in the x , y , and z directions and

$$|l, m, n\rangle \equiv [|l, m, n\rangle_{\uparrow}, |l, m, n\rangle_{\downarrow}] \quad (5)$$

represents the two-component state vector with \uparrow, \downarrow corresponding to the spin degree of freedom. The 2×2 matrices are

$$h_0 = \begin{bmatrix} 2t \cos(k_0 a) + 4B & 0 \\ 0 & -2t \cos(k_0 a) - 4B \end{bmatrix}, \quad (6)$$

$$h_x = \begin{bmatrix} -B & \frac{i}{2}A \\ \frac{i}{2}A & B \end{bmatrix}, \quad (7)$$

$$h_y = \begin{bmatrix} -B & \frac{1}{2}A \\ -\frac{1}{2}A & B \end{bmatrix}, \quad (8)$$

$$h_z = \begin{bmatrix} -t + i\gamma & 0 \\ 0 & t + i\gamma \end{bmatrix}, \quad (9)$$

where $0 < k_0 < \pi/a$, and the other parameters, A , B , t , and γ , are assumed to be real and positive. The Fourier transform of H is expressed as

$$\mathcal{H}(\mathbf{k}) = \begin{bmatrix} \Lambda(\mathbf{k}) + 2\gamma \sin(k_z a) & \Theta_{-}(k_x, k_y) \\ \Theta_{+}(k_x, k_y) & -\Lambda(\mathbf{k}) + 2\gamma \sin(k_z a) \end{bmatrix}, \quad (10)$$

where $\Lambda(\mathbf{k}) = \Delta(k_z) + 2B \sum_{\alpha=x,y} [1 - \cos(k_{\alpha} a)]$ and $\Theta_{\pm}(k_x, k_y) = A[\sin(k_x a) \pm i \sin(k_y a)]$ with

$$\Delta(k_z) = -2t [\cos(k_z a) - \cos(k_0 a)]. \quad (11)$$

It can be seen that inversion symmetry is broken if $\gamma \neq 0$. The energy dispersion of this model is given as

$$E = 2\gamma \sin(k_z a) \pm \left\{ A^2 (\sin^2(k_x a) + \sin^2(k_y a)) + [\Delta(k_z) + 2B(2 - \cos(k_x a) - \cos(k_y a))]^2 \right\}^{\frac{1}{2}}, \quad (12)$$

indicating that a pair of Weyl nodes appears at $\mathbf{k}_{\pm} = (0, 0, \pm k_0)$. Note that $E = 0$ at the band center. The energy of each Weyl node is located at the band center of $E = 0$ at $\gamma = 0$, whereas it deviates from there if $\gamma \neq 0$. In Sect. 4, we focus on the lattice system of a rectangular parallelepiped with L sites in both the x and y directions and N sites in the z direction (see Fig. 1). In this setup, chiral surface states appear on its side.

Now, we show that no spontaneous charge current appears if E_F is located at the band center on the basis of

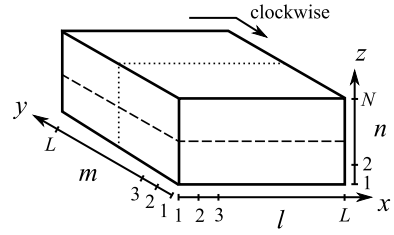


Fig. 1. Lattice system considered in the text: a rectangular parallelepiped with L sites in both the x and y directions and N sites in the z direction.

the particle-hole symmetry inherent in the model introduced above. Let us define the operator Γ_{ph} as

$$\Gamma_{\text{ph}} = \sigma_x K, \quad (13)$$

where σ_x and K are respectively the x component of the Pauli matrices and the complex conjugate operator. The tight-binding Hamiltonian H satisfies

$$\Gamma_{\text{ph}}^{-1} H \Gamma_{\text{ph}} = -H. \quad (14)$$

Let us denote eigenstates of H in the valence band as $|q\rangle_v$ and those in the conduction band as $|q\rangle_c$ with $q = 1, 2, 3, \dots$, where $H|q\rangle_v = \epsilon_q^v |q\rangle_v$ with $\epsilon_q^v < 0$ and $H|q\rangle_c = \epsilon_q^c |q\rangle_c$ with $\epsilon_q^c > 0$. Here, q labels the eigenstates in descending order (i.e., $0 \geq \epsilon_1^v \geq \epsilon_2^v \geq \epsilon_3^v \geq \dots$) in the valence band and in ascending order (i.e., $0 \leq \epsilon_1^c \leq \epsilon_2^c \leq \epsilon_3^c \leq \dots$) in the conduction band. Equation (14) allows us to set $\epsilon_q^v = -\epsilon_q^c$ with

$$|q\rangle_c = \Gamma_{\text{ph}} |q\rangle_v. \quad (15)$$

We introduce the charge current operator j_{α} defined on an arbitrary site, where $\alpha = x, y, z$ specifies the direction of flow. For example, the current operator j_x on the (l, m, n) th site is given by

$$j_x = -e(-i)[|l+1, m, n\rangle h_x \langle l, m, n| - \text{h.c.}]. \quad (16)$$

It may be more appropriate to state that this is defined on the link connecting the (l, m, n) th and $(l+1, m, n)$ th sites. We can show that any j_{α} is invariant under the transformation of Γ_{ph} as

$$\Gamma_{\text{ph}}^{-1} j_{\alpha} \Gamma_{\text{ph}} = j_{\alpha}. \quad (17)$$

In the ground state with $E_F = 0$, the expectation value of any j_{α} is expressed as

$$\langle j_{\alpha} \rangle = \sum_{q \geq 1} v \langle q | j_{\alpha} | q \rangle_v. \quad (18)$$

By using the relations given above and the completeness of the set of eigenstates consisting of $\{|q\rangle_v\}$ and $\{|q\rangle_c\}$, we can show that

$$\begin{aligned} \langle j_{\alpha} \rangle &= \frac{1}{2} \sum_{q \geq 1} [v \langle q | j_{\alpha} | q \rangle_v + c \langle q | j_{\alpha} | q \rangle_c] \\ &= \frac{1}{2} \text{tr}\{j_{\alpha}\} = 0, \end{aligned} \quad (19)$$

indicating that a spontaneous charge current completely vanishes everywhere in the system at $E_F = 0$. That is, although chiral surface states carry a circulating charge

current, their contribution is completely canceled out by that from bulk states.

Note that the above argument based on particle-hole symmetry is not restricted to the two-orbital model used in this study and is also applicable to the four-orbital model introduced in Ref. 20.

3. Analytical Approach

Before performing numerical simulations in the case of $E_F \neq 0$, we analytically study the behaviors of chiral surface states in a cylindrical Weyl semimetal. To do so, we apply the analytical approach given in Ref. 21, which was developed to describe unusual electron states in a Weyl semimetal: chiral surface states²²⁾ and chiral modes along a screw dislocation.^{23,24)} It is convenient to modify the tight-binding Hamiltonian by taking the continuum limit in the x and y directions, leaving the lattice structure in the z direction so that the resulting model has a layered structure. After the partial Fourier transformation in the z direction, the Hamiltonian is reduced to

$$\mathcal{H} = \begin{bmatrix} \tilde{\Lambda} + 2\gamma \sin(k_z a) & \tilde{A}(\hat{k}_x - i\hat{k}_y) \\ \tilde{A}(\hat{k}_x + i\hat{k}_y) & -\tilde{\Lambda} + 2\gamma \sin(k_z a) \end{bmatrix}, \quad (20)$$

where $\tilde{\Lambda} = \Delta(k_z) + \tilde{B}(\hat{k}_x^2 + \hat{k}_y^2)$ with $\hat{k}_x = -i\partial_x$, $\hat{k}_y = -i\partial_y$, $\tilde{A} = Aa$, and $\tilde{B} = Ba^2$. We adapt this model to a cylindrical Weyl semimetal of radius R by using the cylindrical coordinates (r, ϕ) with $r = \sqrt{x^2 + y^2}$ and $\phi = \arctan(y/x)$. Let $\Psi(r, \phi) = {}^t(F, G)$ be an eigenfunction of \mathcal{H} for a given k_z . It is convenient to rewrite F and G as $F = e^{i\lambda\phi} f(r)$ and $G = e^{i(\lambda+1)\phi} g(r)$, where λ is the azimuthal quantum number. Then, in terms of $\psi(r, \phi) = {}^t(f, g)$ for given k_z and λ , the eigenvalue equation is written as

$$\begin{bmatrix} \Delta(k_z) - \tilde{B}\mathcal{D}_\lambda & \tilde{A}(-i\partial_r - i\frac{\lambda+1}{r}) \\ \tilde{A}(-i\partial_r + i\frac{\lambda}{r}) & -\Delta(k_z) + \tilde{B}\mathcal{D}_{\lambda+1} \end{bmatrix} \psi = \tilde{E}\psi, \quad (21)$$

where $\tilde{E} = E - 2\gamma \sin(k_z a)$ and

$$\mathcal{D}_\lambda = \partial_r^2 + \frac{1}{r}\partial_r - \frac{\lambda^2}{r^2}. \quad (22)$$

As demonstrated in Ref. 21, if \tilde{B} is finite but very small, the eigenvalue equation, Eq. (21), can be decomposed into two separate equations: the Weyl and supplementary equations. The Weyl equation for f and g is given by

$$(\mathcal{D}_\lambda - \Lambda_-)f = 0, \quad (\mathcal{D}_{\lambda+1} - \Lambda_-)g = 0, \quad (23)$$

while the supplementary equation is

$$(\mathcal{D}_\lambda - \Lambda_+)f = 0, \quad (\mathcal{D}_{\lambda+1} - \Lambda_+)g = 0, \quad (24)$$

where

$$\Lambda_- = -\frac{\tilde{E}^2 - \Delta^2}{\tilde{A}^2}, \quad \Lambda_+ = \frac{\tilde{A}^2}{\tilde{B}^2}. \quad (25)$$

Here, f and g are related by the original eigenvalue equation with a finite but very small \tilde{B} . Note that the restriction on \tilde{B} (i.e., \tilde{B} is very small) does not significantly affect the behaviors of chiral surface states. Indeed, the energy of chiral surface states does not depend on \tilde{B} as seen in Eq. (28).

We hereafter focus on chiral surface states, which appear only in the case of $|\Delta(k_z)| > |\tilde{E}|$. The solutions of both the Weyl and supplementary equations are expressed by modified Bessel functions in this case. By superposing two solutions that asymptotically increase in an exponential manner, we can describe spatially localized states near the side. With $\eta \equiv \sqrt{\Delta^2 - \tilde{E}^2}/\tilde{A}$ and $\kappa \equiv \tilde{A}/\tilde{B}$, the general solution for given λ and k_z is written as

$$\psi = a \begin{bmatrix} I_{|\lambda|}(\eta r) \\ -i\frac{\Delta - \tilde{E}}{\sqrt{\Delta^2 - \tilde{E}^2}} I_{|\lambda+1|}(\eta r) \end{bmatrix} + b \begin{bmatrix} I_{|\lambda|}(\kappa r) \\ iI_{|\lambda+1|}(\kappa r) \end{bmatrix}, \quad (26)$$

where the first and second terms respectively arise from the Weyl and supplementary equations. The boundary condition of $\psi(R) = {}^t(0, 0)$ requires

$$\frac{\Delta - \tilde{E}}{\sqrt{\Delta^2 - \tilde{E}^2}} = -\frac{I_{|\lambda+1|}(\kappa R)}{I_{|\lambda|}(\kappa R)} \frac{I_{|\lambda|}(\eta R)}{I_{|\lambda+1|}(\eta R)}, \quad (27)$$

indicating that a relevant solution is obtained only in the case of $\Delta(k_z) < 0$, which holds when $k_z \in (-k_0, k_0)$. The eigenvalue of energy is approximately determined as

$$E = \frac{\tilde{A}}{R} \left(\lambda + \frac{1}{2} \right) + 2\gamma \sin(k_z a). \quad (28)$$

In the case of $\gamma = 0$, the dispersion is flat (i.e., independent of k_z), representing a characteristic feature of the chiral surface state. An electron in the chiral surface state propagates in the anticlockwise direction viewed from above. The dispersion becomes dependent on k_z if $\gamma \neq 0$, indicating that the group velocity is tilted to the z direction. Consequently, an electron in the chiral surface state circulates around the side surface in a spiral manner.¹⁹⁾ This implies that a spontaneous charge current in the z direction can be induced near the side surface if $\gamma \neq 0$.

Now, we roughly determine the magnitude of a spontaneous circulating current in the system consisting of N layers. The circulating charge current carried by each chiral surface state is

$$J_\phi^0 = -e\frac{\tilde{A}}{2\pi R}, \quad (29)$$

which flows in the clockwise direction. Note that the chiral surface state with $E(\lambda)$ appears only when $k_z \in (-k_0, k_0)$. If k_z deviates from this interval, the state is continuously transformed to a bulk state, which is spatially extended over the entire system. Let us determine the total charge current J_ϕ . Since J_ϕ vanishes at $E_F = 0$, we need to collect the contributions to J_ϕ arising from the chiral surface states with $E(\lambda)$ satisfying $0 < E < E_F$ if $E_F > 0$. Here, it is assumed that the contribution from bulk states in the same interval of energy is not important since their wavelength is relatively long and hence they cannot induce a short-wavelength response localized near the surface. If $E_F < 0$, the total charge current is obtained by collecting the contributions to J_ϕ arising from the states with $E(\lambda)$ satisfying $E_F < E < 0$ and then reversing its sign. In addition to the condition for λ , it is important to note that the chiral surface states are

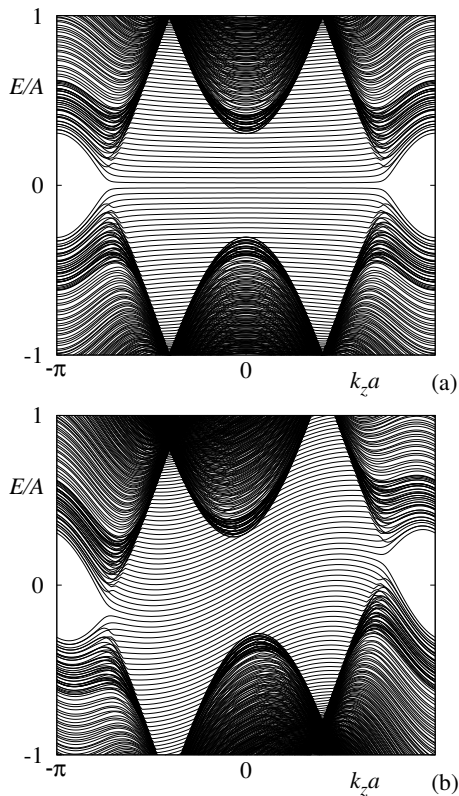


Fig. 2. Energy dispersion as a function of k_z in the cases of (a) $\gamma/A = 0$ and (b) 0.1. For the purely bulk states, only a quarter of the corresponding branches are shown for clarity.

stabilized only when $|k_z| < k_0$. Assuming that k_z is given by $k_z^j = j\pi/[(N+1)a]$ with $j = 1, 2, 3, \dots$ in the system consisting of N layers, we require $k_z^j < k_0$. From the observation given above, we find that the spontaneous charge current per layer is

$$\frac{J_\phi}{N} = -e \frac{k_0 a}{2\pi^2} E_F, \quad (30)$$

which depends on E_F as well as k_0 . This indicates that the direction of flow reverses depending on the sign of E_F . That is, the spontaneous current flows in opposite directions for the cases of electron doping and hole doping. Note that, since J_ϕ/N is independent of R , we expect that the circulating charge current will be insensitive to the geometry of the Weyl semimetal. Thus, we expect that Eq. (30) can be applied to the system of a rectangular parallelepiped, which is treated in the next section.

4. Numerical Results

We focus on the lattice system of the rectangular parallelepiped shown in Fig. 1, which occupies the region of $1 \leq l, m \leq L$ and $1 \leq n \leq N$, under the open boundary condition in the three spatial directions. We set $L = 50$ and $N = 30$ with the following parameters: $B/A = 0.5$, $t/A = 0.5$, and $k_0 a = 3\pi/4$. We consider the cases of $\gamma/A = 0$ and 0.1 for $E_F/A = \pm 0.1$ and ± 0.2 . The energy dispersion for the infinitely long system with a cross-sectional area of L^2 is shown in Fig. 2 in the cases of (a) $\gamma/A = 0$ and (b) 0.1 as a function of k_z . In the case of $\gamma/A = 0$, branches with flat dispersion are uniformly

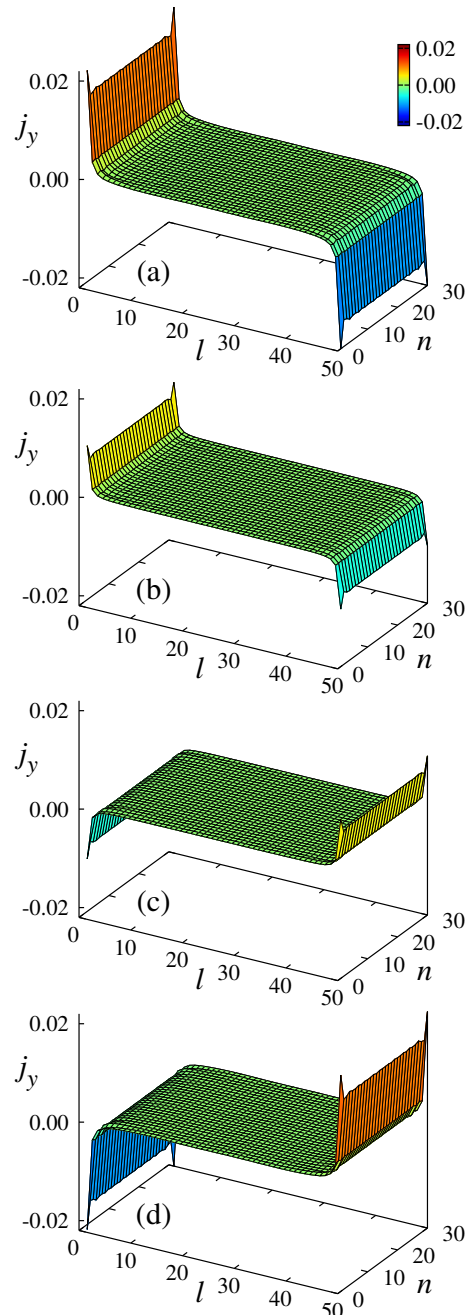


Fig. 3. (Color online) Spatial distribution of j_y normalized by eA in the cross section parallel to the xz plane; (a) $E_F/A = 0.2$, (b) 0.1, (c) -0.1 , and (d) -0.2 .

distributed near $E = 0$ in the region of $-k_0 < k_z < k_0$. They represent chiral surface states localized near the side surface of the system. These states should induce a circulating charge current near the side surface when $E_F \neq 0$. The dispersion of these states becomes slightly upward to the right in the case of $\gamma/A = 0.1$, implying the appearance of a spontaneous charge current in the z direction. Hereafter, we numerically study how the spontaneous charge current appears in this system depending on E_F and γ .

Firstly, let us examine the behaviors of a spontaneous charge current that circulates around the system near the side surface. To do so, we calculate the distribution of the

spontaneous charge current in the y direction through the cross section parallel to the xz plane at the center of the system (dotted line in Fig. 1). Precisely speaking, j_y on each link connecting the $(l, 25, n)$ th and $(l, 26, n)$ th sites is calculated for $1 \leq l \leq 50$ and $1 \leq n \leq 30$. Figure 3 shows the results for j_y normalized by eA for $\gamma/A = 0$ and $E_F/A = 0.2, 0.1, -0.1,$ and -0.2 . The results for $\gamma/A = 0.1$ are not shown since they are almost identical to those for $\gamma/A = 0$. We observe that $j_y > 0$ near $l = 1$ and $j_y < 0$ near $l = 50$ in the case of $E_F > 0$, whereas $j_y < 0$ near $l = 1$ and $j_y > 0$ near $l = 50$ in the case of $E_F < 0$. This indicates that the spontaneous charge current circulates around the system in the clockwise direction viewed from above when $E_F > 0$, whereas it circulates in the anticlockwise direction when $E_F < 0$ (see Fig. 1). That is, its direction of flow is opposite for the cases of $E_F > 0$ and $E_F < 0$. We also observe that j_y increases with increasing E_F in accordance with Eq. (30). Equation (30) predicts $|J_y|/N \approx 0.024 \times eA$ in the case of $E_F/A = \pm 0.2$, where J_y represents the total charge current induced near each side surface of height N . This result is consistent with those shown in Figs. 3(a) and 3(d).

Secondly, let us examine the behaviors of a spontaneous charge current in the longitudinal direction. We calculate the distribution of the charge current in the z direction through the cross section parallel to the xy plane at the center of the system (broken line in Fig. 1). Precisely speaking, j_z on each link connecting the $(l, m, 15)$ th and $(l, m, 16)$ th sites is calculated for $1 \leq l \leq 50$ and $1 \leq m \leq 50$. Figure 4 shows the results for j_z normalized by eA for $\gamma/A = 0.1$ and $E_F/A = 0.2, 0.1, -0.1,$ and -0.2 . The results for $\gamma/A = 0$ are not shown since j_z vanishes everywhere in this case. Again, Fig. 4 indicates that j_z increases with increasing E_F and that its sign is opposite for the cases of $E_F > 0$ and $E_F < 0$. Note that a relatively large current appears near the side surface, particularly near the corners, while a small current flowing in the opposite direction is distributed beneath the side surface. The former is induced by chiral surface states, while the latter originates from bulk states. These two contributions cancel each other out if they are integrated over the cross section; thus, the total charge current in the z direction completely vanishes.

Finally, we examine the effect of disorder^{25–30} on the spontaneous charge current by adding the impurity potential term

$$H_{\text{imp}} = \sum_{l,m,n} |l, m, n\rangle \begin{bmatrix} V_1^{(l,m,n)} & 0 \\ 0 & V_2^{(l,m,n)} \end{bmatrix} \langle l, m, n| \quad (31)$$

to the Hamiltonian H , where V_1 and V_2 are assumed to be uniformly distributed within the interval of $[-W/2, +W/2]$. Previous studies have shown that a Weyl semimetal phase is robust against weak disorder up to a critical disorder strength, W_c ,^{25,26} and that chiral surface states also persist as long as $W < W_c$.²⁹ In the case of $B/A = 0.5$, $t/A = 0.5$, and $k_0a = 3\pi/4$, the critical disorder strength is $W_c/A \sim 4$. The ensemble

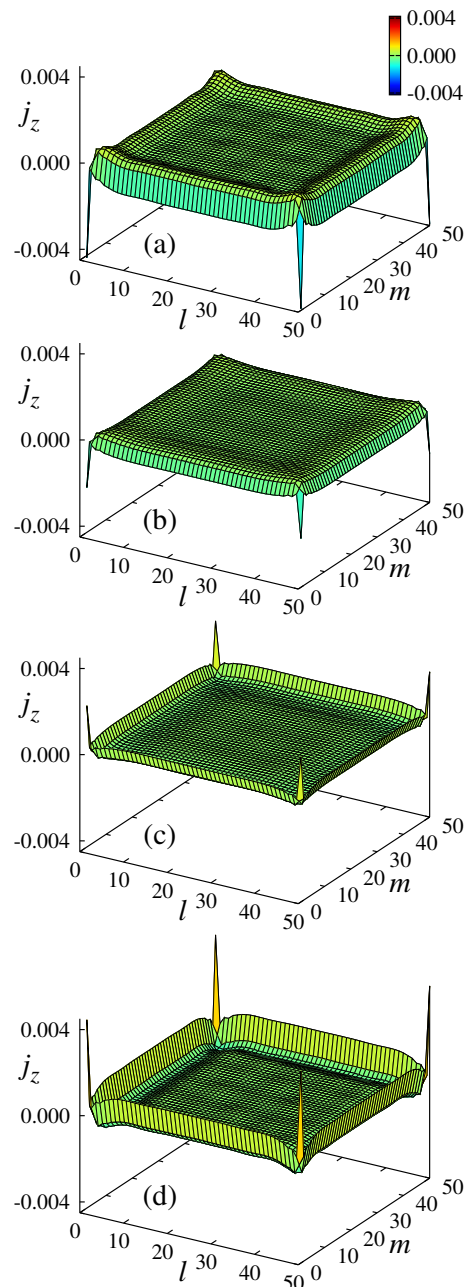


Fig. 4. (Color online) Spatial distribution of j_z normalized by eA in the cross section parallel to the xy plane; (a) $E_F/A = 0.2$, (b) 0.1 , (c) -0.1 , and (d) -0.2 .

averages, $\langle j_y \rangle$ and $\langle j_z \rangle$, are calculated over 500 samples with different impurity configurations at $E_F/A = 0.1$ for a given value of W/A . In calculating j_y and j_z for a given impurity configuration, we take account of only the contribution from electron states with an energy E satisfying $0 < E < E_F$, assuming that electron states below the band center have no contribution owing to cancellation between them. This assumption is not strictly justified here since particle-hole symmetry is broken by the impurity potential. Nonetheless, this should be a good approximation after taking the ensemble average.

Figure 5 shows the results for $\langle j_y \rangle$ normalized by eA for $\gamma/A = 0$ and $E_F/A = 0.1$ with $W/A = 3, 4,$ and 4.5 . We observe that the circulating charge current is ro-

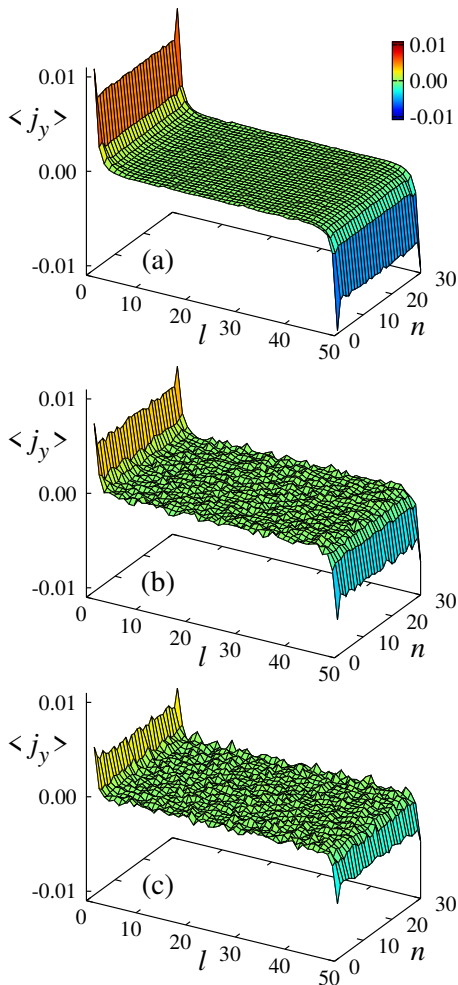


Fig. 5. (Color online) Spatial distribution of $\langle j_y \rangle$ normalized by eA in the cross section parallel to the xz plane at $E_F/A = 0.1$; (a) $W/A = 3$, (b) 4, and (c) 4.5.

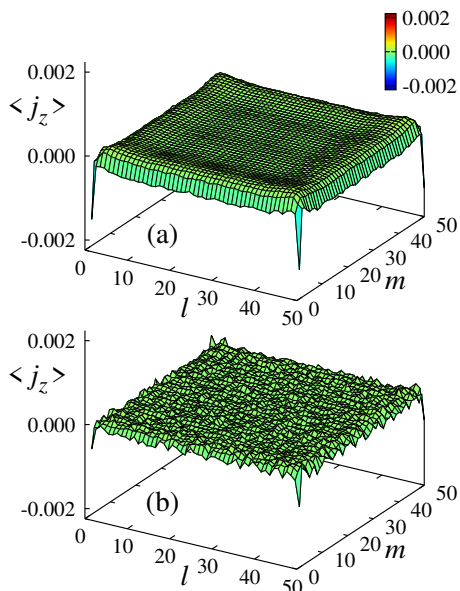


Fig. 6. (Color online) Spatial distribution of $\langle j_z \rangle$ normalized by eA in the cross section parallel to the xy plane at $E_F/A = 0.1$; (a) $W/A = 2$, and (b) 3.

bust against disorder up to $W/A \sim 4$ but is suppressed when W/A exceeds 4. This behavior is consistent with an observation reported previously.²⁹⁾ Figure 6 shows the results for $\langle j_z \rangle$ normalized by eA for $\gamma/A = 0.1$ and $E_F/A = 0.1$ with $W/A = 2$ and 3. We observe that $\langle j_z \rangle$ is significantly suppressed in the case of $W/A = 3$, although the circulating charge current is almost unaffected in this case. This indicates that the charge current in the z direction is more fragile than the circulating charge current against the mixing of chiral surface states and bulk states due to disorder.

5. Summary and Discussion

We theoretically studied a spontaneous charge current due to chiral surface states in the ground state of a Weyl semimetal. We analytically and numerically determined the magnitude of the charge current induced near the side surface of the system. It is shown that no spontaneous charge current appears when the Fermi level, E_F , is located at the band center. It is also shown that, once E_F deviates from the band center, the spontaneous charge current appears to circulate around the side surface of the system and its direction of flow is opposite for the cases of electron doping and hole doping. The circulating current is shown to be robust against weak disorder.

Let us focus on the two features revealed in this paper: the appearance of a spontaneous charge current except at the band center and the reversal of its direction of flow as a function of E_F . As they are derived by using a model possessing particle-hole symmetry, a natural question arises: do these features manifest themselves even in the absence of particle-hole symmetry? The answer is yes. The disappearance of the spontaneous charge current reflects the fact that the contribution from chiral surface states is completely canceled out by that from bulk states. As the spontaneous charge current due to chiral surface states is localized near the side surface, this cancellation should be mainly caused by bulk states with a short wavelength, occupying the bottom region of the energy band far from the band center. Hence, if E_F is varied near the band center, the contribution from bulk states is almost unaffected but that from chiral surface states is significantly changed, depending on E_F in a roughly linear manner. This behavior should take place regardless of the presence or absence of particle-hole symmetry. Thus, we expect that the features of the spontaneous charge current still manifest themselves even in the absence of particle-hole symmetry, although the point of the disappearance shifts away from the band center.

Acknowledgment

This work was supported by JSPS KAKENHI Grant Numbers JP15K05130 and JP18K03460.

- 1) R. Shindou and N. Nagaosa, Phys. Rev. Lett. **87**, 116801 (2001).
- 2) S. Murakami, New J. Phys. **9**, 356 (2007).
- 3) X. Wan, A. M. Turner, A. Vishwanath, and S. Y. Savrasov, Phys. Rev. B **83**, 205101 (2011).
- 4) K.-Y. Yang, Y.-M. Lu, and Y. Ran, Phys. Rev. B **84**, 075129

- (2011).
- 5) A. A. Burkov and L. Balents, *Phys. Rev. Lett.* **107**, 127205 (2011).
 - 6) A. A. Burkov, M. D. Hook, and L. Balents, *Phys. Rev. B* **84**, 235126 (2011).
 - 7) W. Witczak-Krempa and Y. B. Kim, *Phys. Rev. B* **85**, 045124 (2012).
 - 8) P. Delpace, J. Li, and D. Carpentier, *Europhys. Lett.* **97**, 67004 (2012).
 - 9) G. Halász and L. Balents, *Phys. Rev. B* **85**, 035103 (2012).
 - 10) A. Sekine and K. Nomura, *J. Phys. Soc. Jpn.* **82**, 033702 (2013).
 - 11) H. Weng, C. Fang, Z. Fang, B. A. Bernevig, and X. Dai, *Phys. Rev. X* **5**, 011029 (2015).
 - 12) S.-M. Huang, S.-Y. Xu, I. Belopolski, C.-C. Lee, G. Chang, B. Wang, N. Alidoust, G. Bian, M. Neupane, C. Zhang, S. Jia, A. Bansil, H. Lin, and M. Z. Hasan, *Nat. Commun.* **6**, 7373 (2015).
 - 13) S.-Y. Xu, I. Belopolski, N. Alidoust, M. Neupane, G. Bian, C. Zhang, R. Sankar, G. Chang, Z. Yuan, C.-C. Lee, S.-M. Huang, H. Zheng, J. Ma, D. S. Sanchez, B. Wang, A. Bansil, F. Chou, P. P. Shibayev, H. Lin, S. Jia, and M. Z. Hasan, *Science* **349**, 613 (2015).
 - 14) B.-Q. Lv, H.-M. Weng, B.-B. Fu, X.-P. Wang, H. Miao, J. Ma, P. Richard, X.-C. Huang, L.-X. Zhao, G.-F. Chen, Z. Fang, X. Dai, T. Qian, and H. Ding, *Phys. Rev. X* **5**, 031013 (2015).
 - 15) B. Q. Lv, N. Xu, H. M. Weng, J. Z. Ma, P. Richard, X. C. Huang, L. X. Zhao, G. F. Chen, C. E. Matt, F. Bisti, V. N. Strocov, J. Mesot, Z. Fang, X. Dai, T. Qian, M. Shi, and H. Ding, *Nat. Phys.* **11**, 724 (2015).
 - 16) S.-Y. Xu, N. Alidoust, I. Belopolski, Z. Yuan, G. Bian, T.-R. Chang, H. Zheng, V. N. Strocov, D. S. Sanchez, G. Chang, C. Zhang, D. Mou, Y. Wu, L. Huang, C.-C. Lee, S.-M. Huang, B. Wang, A. Bansil, H.-T. Jeng, T. Neupert, A. Kaminski, H. Lin, S. Jia, and M. Z. Hasan, *Nat. Phys.* **11**, 748 (2015).
 - 17) S. Souma, Z. Wang, H. Kotaka, T. Sato, K. Nakayama, Y. Tanaka, H. Kimizuka, T. Takahashi, K. Yamauchi, T. Oguchi, K. Segawa, and Y. Ando, *Phys. Rev. B* **93**, 161112 (2016).
 - 18) K. Kuroda, T. Tomita, M.-T. Suzuki, C. Bareille, A. A. Nugroho, P. Goswami, M. Ochi, M. Ikhlas, M. Nakayama, S. Akebi, R. Noguchi, R. Ishii, N. Inami, K. Ono, H. Kumigashira, A. Varykhalov, T. Muro, T. Koretsune, R. Arita, S. Shin, T. Kondo, and S. Nakatsuji, *Nat. Mater.* **16**, 1090 (2017).
 - 19) P. Baireuther, J. A. Hutasoit, J. Tworzydło, and C. W. J. Beenakker, *New J. Phys.* **18**, 045009 (2016).
 - 20) M. M. Vazifeh and M. Franz, *Phys. Rev. Lett.* **111**, 027201 (2013).
 - 21) Y. Takane, *J. Phys. Soc. Jpn.* **86**, 123708 (2017).
 - 22) R. Okugawa and S. Murakami, *Phys. Rev. B* **89**, 235315 (2014).
 - 23) K.-I. Imura and Y. Takane, *Phys. Rev. B* **84**, 245415 (2011).
 - 24) H. Sumiyoshi and S. Fujimoto, *Phys. Rev. Lett.* **116**, 166601 (2016).
 - 25) C.-Z. Chen, J. Song, H. Jiang, Q.-F. Sun, Z. Wang, and X. C. Xie, *Phys. Rev. Lett.* **115**, 246603 (2015).
 - 26) H. Shapourian and T. L. Hughes, *Phys. Rev. B* **93**, 075108 (2016).
 - 27) S. Liu, T. Ohtsuki, and R. Shindou, *Phys. Rev. Lett.* **116**, 066401 (2016).
 - 28) E. V. Gorbar, V. A. Miransky, I. A. Shovkovy, and P. O. Sukhachov, *Phys. Rev. B* **93**, 235127 (2016).
 - 29) Y. Takane, *J. Phys. Soc. Jpn.* **85**, 124711 (2016).
 - 30) Y. Yoshimura, W. Onishi, K. Kobayashi, T. Ohtsuki, and K.-I. Imura, *Phys. Rev. B* **94**, 235414 (2016).